Effect of peptide-chelate architecture on the metabolic stability of peptide-based MRI contrast agents

Zhaoda Zhang,[a] Andrew F. Kolodziej,[b] Jianfeng Qi,[b] Shrikumar A. Nair,[b] Xifang Wang,[b] April W. Case,[b] Matthew T. Greenfield,[b] Philip B. Graham,[b] Thomas J. McMurry[b] and Peter Caravan*[a]

Received (in Gainesville, FL, USA) 23rd December 2009, Accepted 15th January 2010
First published as an Advance Article on the web 12th February 2010
DOI: 10.1039/b9nj00787c

A strategy for preparing high relaxivity, metabolically-stable, peptide-based MR contrast agents is described.

The chemical and topological diversity of peptides offers tremendous possibilities for identifying new diagnostic imaging compounds. Peptides have been widely used to target imaging probes to specific proteins or receptors, and thereby provide greater specificity. Typically, an imaging reporting moiety (*e.g.* positron emitter, gamma emitter, paramagnetic ion or near-infrared fluorophore) is conjugated to the peptide. The site of conjugation, the linker and the type of imaging reporter all play a role in determining biological activity and pharmacokinetics.[1,2] For peptide-based magnetic resonance imaging (MRI) contrast agents, an additional factor is the detection sensitivity of the imaging probe.[3] Multiple copies of the MR active reporter, typically a gadolinium complex, are required to provide robust image contrast.

An additional major challenge to creating new drugs from peptides is peptide degradation by endogenous peptidases. There are numerous medicinal chemistry approaches for improving peptide stability, biological activity and/or bioavailability that increase in complexity from modified peptides to pseudopeptides to small molecule peptidomimetics.[4,5] In this Letter, we explore the potential of using an imaging reporter to block peptidase activity.

We[6–9] and others[10–14] have been interested in developing gadolinium-based peptide-targeted MRI agents. Compared to other modalities, MRI provides a favorable combination of high spatial resolution, depth penetration and a lack of ionizing radiation. Unlike nanoparticles, these relatively small molecules can rapidly reach targets in extravascular spaces and can be readily excreted through the kidneys to reduce/avoid long-term gadolinium retention and toxicity. On the other hand, extravasation into the kidneys and liver exposes these compounds to a range of peptidases.

There is some flexibility as to where and how the gadolinium chelates are conjugated to the peptide. Conjugation is possible at the N- or C-terminus and/or within the peptide structure.[6] We recently reported some fibrin-specific peptides conjugated with one or four $[Gd(DTPA)]^{2-}$ moieties.[8] The construct with the highest affinity had two peptides linked *via* their N-terminus to a GdDTPA tetramer, *i.e.* Pep^{N}-Gd_4-^{N}Pep, termed EP-1084 (compound **1** in Scheme 1). **1** showed good fibrin affinity and specificity, high relaxivity, and positive uptake in an *in vivo* venous thrombus model. However, subsequent *in vivo* studies revealed that this compound was being metabolized over the course of the study, and that the gadolinium-containing metabolites no longer bound fibrin. This Letter describes our efforts to improving the metabolic

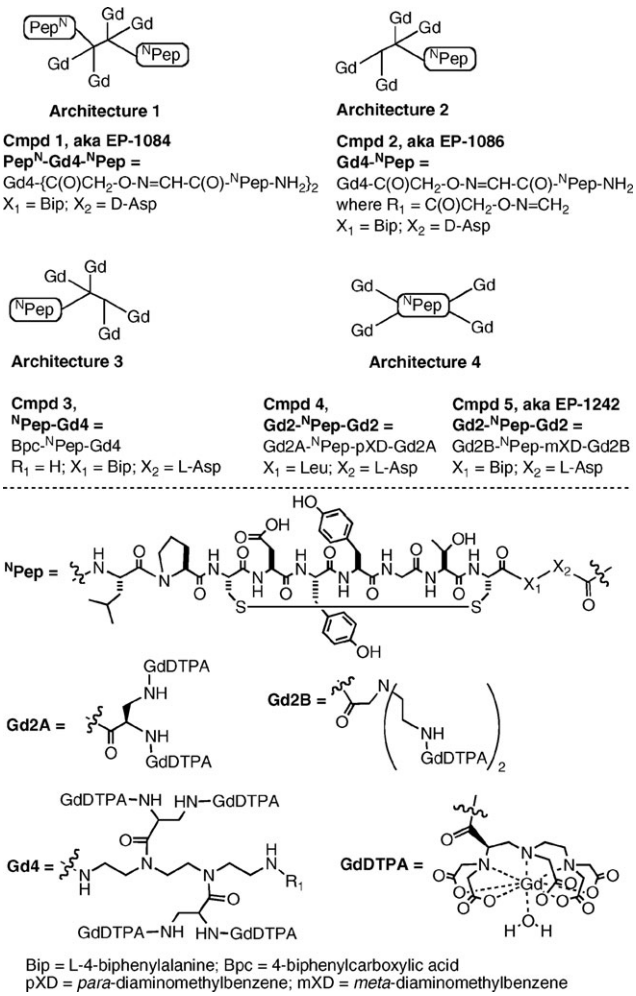

Scheme 1 The compounds used in this study.

[a] *A. A. Martinos Center for Biomedical Imaging, Massachusetts General Hospital and Harvard Medical School, 149 Thirteenth St., Suite 2301, Charlestown, MA 02129, USA. E-mail: caravan@nmr.mgh.harvard.edu*
[b] *Epix Pharmaceuticals, 4 Maguire Road, Lexington, MA 02140, USA*

stability of this class of compounds while maintaining their biological and relaxometric activity. We demonstrate that the gadolinium chelate moieties can be used to block peptidase activity, in addition to their role in MRI signal generation. Parts of this work have been communicated previously in conference abstracts.[15,16]

Scheme 1 shows the compounds described in this Letter, which use three similar peptides, differing only at the C-terminus. The L-Asp to D-Asp substitution did not affect fibrin affinity, but D-amino acids are known to sometimes provide metabolic stability.[4] The Leu to biphenylalanine (Bip) substitution resulted in higher fibrin affinity,[8] and it was hoped that the unnatural amino acid would improve stability. Peptides are linked to the gadolinium chelates *via* an oxime or amide bond.

A typical *in vitro* assay for metabolism is to incubate the compound with tissue homogenate or liver microsomes. Rat liver homogenate consists of a mixture of proteases and other enzymes, and represents a harsh challenge to compound stability. The half-life of **1** in liver homogenate at 37 °C was 10.8 min, which was consistent with the observed instability *in vivo*. The peptides alone, with or without the Bip or D-Asp substitutions, were completely metabolized within the time taken for measurement, $t_{\frac{1}{2}} < 2$ min. The bulky hydrophilic GdDTPA tetramer at the N-terminus appeared to block metabolism. This was supported by studies with single peptide analog **2** (Gd4-^{N}Pep). The half-life of this compound was similar to **1** (10.0 min, Table 1), suggesting that blockading of the C-terminus might be required for enhanced stability. Compound **3** (Bpc-^{N}Pep-Gd4) was synthesized with the gadolinium tetramer conjugated directly to the C-terminus and the N-terminus capped with biphenyl carboxamide (Bpc), a group used to block exopeptidase activity. However, this compound also had a similar half-life in rat liver homogenate (9 min). With compound **4**, we took this strategy further and capped the C- and N-termini with a GdDTPA dimeric unit (Gd2A-^{N}-Pep-Gd2A), resulting in a six- to seven-fold increase in metabolic stability. This suggests that while the D-amino acid and unnatural Bip in **2**, and the Bpc in **3**, may increase stability, these substitutions are not as effective as using the metal chelate with this specific peptide.

While the metabolic stability was improved with compound **4**, unfortunately, its fibrin affinity was significantly reduced. Table 1 also shows inhibition constants, K_i, for each compound to inhibit the binding of a fluorescent peptide to the soluble fibrin fragment DD(E). A lower K_i value indicates higher fibrin affinity. The K_i values for **1** and **2** are comparable to the binding dissociation constants to insoluble fibrin reported previously (for **1**, K_i (DD(E)) = 1.1 μM, K_d (fibrin) = 1.9 μM). To improve the fibrin affinity of metabolically-stable **4**, we made the Leu to Bip substitution used in **1** to give compound **5** (Gd2B-Pep-Gd2B), which resulted in a two- to three-fold increase in fibrin affinity while maintaining the metabolic stability. The other modifications from **4** to **5** were practical: the *meta*-bis-(aminomethyl)-benzene linker was much less expensive than the *para* analog and the bis(GdDTPA) moiety Gd2B prepared from diethylene triamine gave better yields than Gd2A prepared from diaminopropionic acid. Although the affinity of **5** was still less than that of **1**, it was a simpler and more cost-effective molecule, utilizing only one peptide per compound. Compound **5** (aka EP-1242) subsequently showed efficacy in a guinea pig model of arterial thrombosis.[17]

Based on its favorable fibrin affinity and metabolic stability properties, we sought to further characterize the MR properties of **5**. Nuclear magnetic relaxation dispersion (NMRD) profiles of **5** in either pH 7.4 Tris buffered saline (TBS), a 30 μM human fibrinogen/TBS solution, human plasma or 30 μM gelled human fibrin in TBS are shown in Fig. 1. The large enhancement in relaxivity in going from TBS to fibrin, and the peak in relaxivity at *ca.* 30 MHz, are consistent with binding to fibrin and a reduction in the rotational correlation time (τ_R). There was little relaxivity enhancement in the fibrinogen solution, suggesting that **5** does not bind or binds weakly to fibrinogen. Some enhanced relaxivity in the plasma suggests some weak binding to plasma proteins. Relaxivity in Fig. 1 is plotted on a per-molecule basis to demonstrate the increased detection sensitivity of **5** compared to commercial $[Gd(DTPA)]^{2-}$.

Fig. 2 shows the dual effect of fibrin targeting and relaxation enhancement on thrombus imaging. Two 500 μL solutions were prepared, each containing 30 μM compound **5** in fibrinogen enriched (10 mg mL^{-1}) human plasma. One sample was clotted by the addition of 4 μL of a 2 M $CaCl_2$ solution and 2 μL of human thrombin (0.6 units). After clotting, the clot

Table 1 The effect of peptide chelate architecture on metabolic stability, as assessed by the half-life ($t_{\frac{1}{2}}$) in rat liver homogenate, and affinity to DD(E) (soluble fibrin fragment)

Compound	Architecture	$t_{\frac{1}{2}}{}^{a}$/min	K_i/μM[a]
1 (EP-1084)	PepN-Gd4-NPep	10.8	1.1
2 (EP-1086)	Gd4-NPep	10.0	4.7
3	NPep-Gd4	9.0	9.1
4	Gd2-NPep-Gd2	65.2	12.0
5 (EP-1242)	Gd2-NPep-Gd2	>70	4.7

[a] Uncertainties estimated at ±10%.

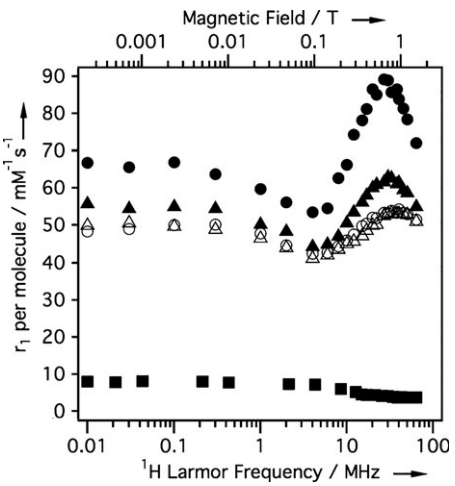

Fig. 1 NMRD showing the field- and medium-dependent relaxivity of **5** at 35 °C in TBS buffer (△), 30 μM human fibrinogen/TBS (○), human plasma (▲) and 30 μM fibrin gel (●). NMRD of $[Gd(DTPA)]^{2-}$ in plasma (■) is shown for reference.

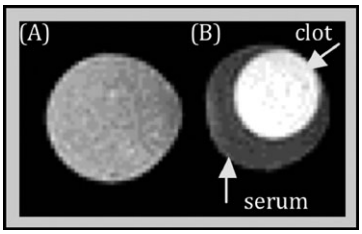

Fig. 2 T1-weighted MR images of **5** in (A) unclotted and (B) clotted human plasma from a 1.5 T clinical scanner (General Electric) with a 6 cm surface coil, using a spoiled gradient echo sequence (TE/TR/α: 3/39/40°).

was allowed to retract by gentle agitation with an Eppendorf pipette tip. Relative to **5** in plasma (Fig. 2(A)), the signal intensity in the clot (Fig. 2(B)) is higher because of the increased concentration of **5** due to binding, and also because of higher relaxivity. The concentration of **5** in the serum is depleted, resulting in a lower signal intensity.

Additional NMRD at 5, 15, 25 and 35 °C for **5** in TBS or in a fibrin gel, and variable temperature O-17 solvent relaxation studies (T_1, T_2) for **5** in TBS, were performed to better understand the underlying dynamics influencing relaxation. Fig. 3 shows the results of these studies, with solid lines as fits to the data. The high field NMRD and O-17 data were analyzed as described previously[18] using the usual Solomon Bloembergen Morgan equations with two-site exchange.[19] The data were well described by an isotropic model of rotation, and the τ_R of this peptide-gadolinium tetramer is substantially increased compared to $[Gd(DTPA)]^{2-}$ (390 ps *vs.* 44 ps[20] at 37 °C), accounting for the increased relaxivity of **5** compared to $[Gd(DTPA)]^{2-}$. Not surprisingly, the water exchange rate and parameters for electronic relaxation at the backbone modified Gd(DTPA)(H_2O) moiety in **5** are very similar to those of $[Gd(DTPA)]^{2-}$ and related derivatives.[18,20]

The lack of temperature dependence on the relaxivity of fibrin-bound **5** implies that there is substantial internal motion

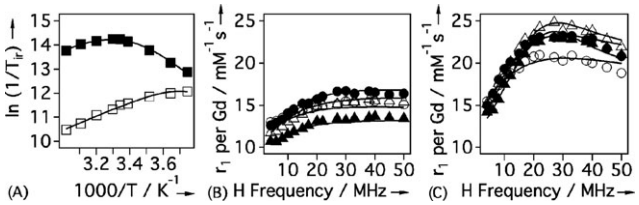

Fig. 3 Relaxometric analysis of **5**: (A) VT O-17 NMR ($1/T_1$ □, $1/T_2$ ■) at 7.05 T in TBS. VT NMRD in (B) TBS and (C) fibrin gel at 5 (○), 15 (●), 25 (△) and 35 (▲) °C. The solid lines are fits to the data.

limiting the relaxivity. If fibrin binding caused true immobilization then the relaxivity should decrease with decreasing temperature, because relaxation would be limited by slow water exchange. The NMRD data of the fibrin-bound **5** was modelled with the Lipari–Szabo formalism, where two correlation times describe rotational diffusion: a slow, global correlation time (τ_R) for the protein-bound compound and a shorter, local correlation time (τ_l) for internal motion.[18,21] These are weighted by an order parameter, $1 \geq F^2 \geq 0$, where $F^2 = 1$ represents isotropic global motion and $F^2 = 0$ represents local motion decoupled from the slow global motion. The NMRD data was well described by adjusting the rotational parameters without changing the electronic relaxation and water exchange parameters from those determined in TBS (Table 2). Best-fits were obtained when the global τ_R was very long, >20 ns. However, F^2 was quite small (0.08), indicating that the relaxivity of fibrin-bound **5** was limited by internal motion. As the temperature is decreased, internal motion is reduced, but this positive effect on relaxivity is offset by a decrease in water exchange rate. The overall effect is a near temperature independence on relaxivity.

The NMRD analysis indicates that relaxivity at 37 °C is not likely to be improved by changing the gadolinium chelate to one with faster water exchange kinetics, since relaxivity at 37 °C is limited by fast internal motion and not water exchange. However, reducing internal motion should have a major impact on increasing the relaxivity at 1.5 T (the field at which the vast majority of clinical MRI scanners operate). Nonetheless, the relaxivity observed for **5** is still quite high: 18 mM^{-1} s^{-1} per Gd and 72 per molecule bound to fibrin at 1.5 T. This is four- to five-fold higher than GdDTPA on a per Gd basis and 18-fold higher per molecule, providing the sensitivity to detect thrombi *in vivo*.

A similar Gd2-Pep-Gd2 design was used in EP-2104R,[9,22] which has been used to detect thrombus by MRI in animal models and human clinical trials.[22] EP-2104R uses a different peptide to the compounds in this report, but its metabolic stability may arise in part because of blocking of both the C- and N-termini with gadolinium chelates.

In summary, the metabolic stability of a fibrin-targeted peptide is greatly increased when gadolinium chelates are positioned at both the C- and N-termini to block exopeptidase activity. Using multiple gadolinium chelates also results in increased molecular relaxivity, although NMRD analyses suggest that relaxivity can be even further increased by reducing internal motion. Using more than one site of chelate conjugation may represent a general strategy to increase the metabolic stability of peptide-targeted imaging agents.

Table 2 Parameters (and their temperature dependence in parentheses) obtained from modelling variable temperature ^1H NMRD and $H_2{}^{17}O$ relaxation data for **5** in TBS or in 30 μM fibrin gel (FBN)[a]

	$\tau_m{}^{37}$ ($\Delta H^{\ddagger}$)	$\tau_R{}^{37}$ ($\Delta E_R{}^{\ddagger}$)	$\tau_v{}^{37}$	$\Delta^2 \times 10^{-18}$	F^2	$\tau_{loc}{}^{37}$ ($\Delta E_l{}^{\ddagger}$)
TBS	124 ± 9 (45.7 ± 1.4)	389 ± 4 (24.9 ± 0.4)	18.0 ± 1.7	10.2 ± 0.5	1	NA
FBN	124[b] (45.7[b])	>20 000 (NA)	18[b]	10.2[b]	0.08 ± 0.02	720 ± 20 (30 ± 2)

[a] Units: correlation times τ have units of ps, except for τ_m, which is in ns; activation energies have units of kJ mol^{-1}; Δ^2 has units of s^2; F^2 is dimensionless. [b] Values fixed to those obtained previously for **5** in the absence of fibrin. NA = not applicable.

Experimental

General procedures for synthesis of the protected peptides

Compounds **1** and **2** were prepared as described previously.[8] Peptides were synthesized on an automated peptide synthesizer: Advanced ChemTech ACT-348 Ω. Standard Fmoc chemistry was used to elongate the peptide on the resin. The linear peptide containing Cys(ACM) residuals on the resin was cyclized with a solution of $Tl(TFA)_3$ (2.2 equiv.) in DMF. The cyclic peptide was cleaved from the resin by treating it several times with 1% TFA/DCM (10–15 mL g^{-1} resin) for 5 min.

Synthesis of tetrakis(DTPA)-3-peptide

The protected cyclic peptide (3-peptide) was prepared by using Fmoc-Asp(OtBu)-SUSRIN resin (0.54 mmol g^{-1}). Molecular weight for $C_{88}H_{125}N_{11}O_{20}S_2$ = 1721.13. MS (ESI) *m*/*z* calc.: 1722.1 $(M + H)^+$; found: 1722.8. 3-Peptide (202 mg, 117 μmol) and tetra(DTPE)-diamine[8] (122 mg, 39 μmol) were dissolved in dichloromethane (25 mL) and DMF (25 mL). DIPEA was added dropwise until the pH measured 9, and DIC (15 mg, 117 μmol) and HOBt (21 mg, 137 μmol) were added to the mixture. The mixture was stirred at room temperature overnight. The solvents were removed under reduced pressure. The crude was purified by RP-HPLC with a C4 column (1% TFA/H_2O–CH_3CN) to provide tetrakis(DTPE)-3-peptide as a white solid (72.6 mg, 15 μmol, 12.9% yield). Molecular weight for $C_{240}H_{397}N_{31}O_{65}S_2$ = 4821.02. MS (ESI) *m*/*z* calc.: 1608.0 $[(M + 3H)/3]^{3+}$; found: 1608.3. Tetrakis(DTPE)-3-peptide (72.6 mg, 15 μmol) was dissolved in dichloromethane (2.0 mL) and anisole (2.0 mL), and the solution was stirred at 4 °C for 10 min. To the solution was added dropwise a concentrated HCl solution (2.0 mL). The mixture was stirred at 4–12 °C for 4 h and then water added to the mixture. The mixture was extracted four times with ether. The aqueous solution was lyophilized to give a crude product that was purified by using RP-HPLC with a C18 column (eluents: 0.1% TFA/H_2O–CH_3CN). The fractions containing the pure product were pooled and lyophilized to give tetrakis(DTPA)-3-peptide as a white foam (21.9 mg, 6.4 μmol, 42.7% yield). Molecular weight for $C_{140}H_{197}N_{31}O_{65}S_2$ = 3418.38. MS (ESI) *m*/*z* calc.: 1710.2 $[(M + 2H)/2]^{2+}$; found: 1710.8.

Synthesis of tetrakis(DTPA)-4-peptide

The protected cyclic peptide (4-peptide) was synthesized by using 1,4-bis-(aminomethyl)-benzene trityl NovaSyn TGT resin (0.32 mmol g^{-1}). Molecular weight for $C_{83}H_{127}N_{13}O_{18}S_2$ = 1657.89. MS (ESI) *m*/*z* calc.: 830.6 $[(M + 2H)/2]^{2+}$; found: 831.0. To a solution of 4-peptide (187 mg, 0.113 mmol) in DMF (40 mL) was added a solution of bis(DTPE)-acid-B[23] (508 mg, 0.338 mmol) in dichloromethane (40 mL), HOBt (60.4 mg, 0.395 mmol), DIPEA (102 mg, 0.789 mmol) and then DIC (42.7 mg, 0.338 mmol). The mixture was stirred at room temperature overnight. The solvents were removed under reduced pressure to give a pale yellow oil, which was purified by using an RP-HPLC with a C4 column (eluents: 0.1% TFA/H_2O–CH_3CN) to give tetrakis(DTPE)-4-peptide as a white solid (210 mg, 0.045 mmol, 40.1% yield): Molecular weight for $C_{229}H_{383}N_{29}O_{64}S_2$ = 4630.78. MS (ESI) *m*/*z* calc: 1544.6 $[(M + 3H)/3]^{3+}$; found: 1545.2. Tetrakis(DTPE)-4-peptide (210 mg, 0.045 mmol) was deprotected using dichloromethane (8.0 mL), anisole (8.0 mL) and a concentrated HCl solution (8.0 mL) to obtain tetrakis(DTPA)-4-peptide as a white foam (55 mg, 0.017 mmol, 38% yield). Molecular weight for $C_{129}H_{183}N_{29}O_{64}S_2$ = 3228.14. MS (ESI) *m*/*z* calc.: 1615.1 $[(M + 2H)/2]^{2+}$; found: 1615.3.

Synthesis of tetrakis(DTPA)-5-peptide

The protected cyclic peptide (5-peptide) was synthesized by using 1,3-bis-(aminomethyl)-benzene trityl NovaSyn TGT resin (0.59 mmol g^{-1}). Molecular weight for $C_{92}H_{129}N_{13}O_{18}S_2$ = 1769.21. MS (ESI) *m*/*z* calc.: 885.61 $[(M + 2H)/2]^{2+}$; found: 885.8. 5-Peptide (1.527 g, 0.863 mmol) and bis(DTPE)-acid-A[23] (2.964 g, 1.90 mmol) were dissolved in dichloromethane (100 mL) and DMF (100 mL). DIPEA (about 0.76 mL) was added dropwise until the pH measured 9, and DIC (240 mg, 1.90 mmol) and HOBt (330 mg, 2.16 mmol) were added to the mixture. The mixture was stirred at room temperature for 2 h. The reaction was monitored using LC/MS. If needed, additional pre-activated bis(DTPE)-acid-A (with DIC, DIPEA and HOBt) was added in one portion, and this was repeated 2 h later. After the reaction was complete, the solvents were removed under reduced pressure and the crude product was purified by using an RP-HPLC to give tetrakis(DTPE)-5-peptide as a pale yellow oil (807 mg, 0.166 mmol, 19.3% yield). Molecular weight for $C_{244}H_{399}N_{31}O_{64}S_2$ = 4851.84. MS (ESI) *m*/*z* calc.: 1618.3 $[(M + 3H)/3]^{3+}$; found 1620.2. Tetrakis(DTPE)-5-peptide (357 mg, 0.074 mmol) was deprotected using dichloromethane (12 mL), anisole (12 mL) and a concentrated HCl solution (12 mL) to obtain tetrakis(DTPA)-5-peptide as a white foam (103 mg, 0.030 mmol, 40.2% yield). Molecular weight for $C_{144}H_{199}N_{31}O_{64}S_2$ = 3452.42. MS (ESI) *m*/*z* calc.: 1727.2 $[(M + 2H)/2]^{2+}$; found: 1727.6.

General procedure for final compound preparation

The final compounds, **3**, **4** and **5**, were each prepared by reacting the respective tetrakis(DTPA)-peptide with gadolinium chloride *in situ*. Each tetrakis(DTPA)-peptide was dissolved in a small volume of distilled, de-ionized water (3 mL), and the pH was adjusted to 6.5 using NaOH. The exact ligand concentration of the solution was determined by photometric titration with standardized gadolinium chloride in 0.02 M xylenol orange (pH 4.9, acetate buffer, monitor at 572 nm). There was a marked increase in absorbance once the end point had been reached. Four equivalents of $GdCl_3 \cdot 6H_2O$ were added to the tetrakis-(DTPA)-peptide solution, and the pH adjusted to 6.5 by the addition of NaOH to give an aqueous solution of the final compound, **3**, **4** or **5**. The exact concentration was determined by ICP-MS and contained no excess gadolinium, as detected by xylenol orange, nor measurable amounts of under-chelated product, as determined by photometric titration.

Rat liver homogenate assay for metabolic stability

Rat liver homogenate was prepared from livers isolated from male Sprague Dawley rats.[24] Freshly prepared rat liver homogenate (630 μL) was placed in a glass test tube and incubated

at 37 °C in a water bath for 4 min. 70 μL of a 1 mM solution of test compound was added to the rat liver homogenate at 37 °C. A 100 μL aliquot of the reaction mixture was removed at time points 0, 5, 15, 30 and 60 min, and mixed with 100 μL of methanol in a microfuge tube to quench the reaction. The quenched reaction mixture was centrifuged for 3 min at 10 000 rpm to pellet the precipitated protein. The supernatant was analyzed by LC-MS to quantify the amount of test compound remaining by comparing the area of the single ion MS peak to that of a series of standards.

DD(E) binding assay

The soluble fibrin fragment DD(E) was prepared as previously described.[25] DD(E) used in this study contained subunits of 61 kD and 72 kD, assigned to fragments E_1 and E_2 present in a roughly 1 : 1 ratio, and 180 kD (fragment DD). Peptide conjugate binding to DD(E) was measured by a fluorescence polarization (FP) assay. The anisotropy (r_{obs}) of 0.1 μM fluorescein-labelled peptide (Fluor-Aca-LPCDYYGTCLD, where Aca = aminocaproic acid) binding to DD(E) (0–20 μM) was measured in TBS. The data were fitted to a single site model, eqn (1), to obtain the dissociation constant, K_d, for the DD(E)·(fluorescent peptide, "Fl") complex and reference values for r_{bd}, the anisotropy of Fl when fully bound to DD(E), and r_{fr}, the anisotropy in solution. K_d for the fluorescent peptide binding to DD(E) was 1.3 ± 0.4 μM.

$$r_{obs} = r_{fr} + \frac{r_{bd} - r_{fr}}{[Fl]_t} \times \frac{([DDE]_t + [Fl]_t + K_d) - \sqrt{([DDE]_t + [Fl]_t + K_d)^2 - 4[Fl]_t[DDE]_t}}{2} \quad (1)$$

Binding of peptide chelate conjugates **1**, **2**, **3**, **4** and **5** to DD(E) was measured by fluorescent peptide displacement. DD(E) (1.5 μM), Fl (1 μM) and competing peptide conjugate (0.1–50 μM) were mixed in TBS·Ca. Sample r_{obs} (100 μL, n = 3 wells) values were measured in a 96-well microplate (Costar, cat. no. 3915) using a Tecan Polarian FP microplate reader (λ_{ex} = 485 nm, λ_{em} = 535 nm). In the presence of inhibitor, an apparent dissociation constant for the fluorescent probe, K_d^{app}, was determined (eqn (2)). The inhibition constant, K_i, is related to K_d^{app} by eqn (3), where K_d is the true dissociation constant of the fluorescent probe measured in the absence of inhibitor. K_i values were obtained by least squares fitting of the data, as described elsewhere.[26]

$$r_{obs} = r_{fr} + \frac{r_{bd} - r_{fr}}{[Fl]_t} \times \frac{([DDE]_t + [Fl]_t + K_d^{app}) - \sqrt{([DDE]_t + [Fl]_t + K_d^{app})^2 - 4[Fl]_t[DDE]_t}}{2} \quad (2)$$

$$K_d^{app} = K_d\left(1 + \frac{[\text{inhibitor}]_{free}}{K_i}\right) \quad (3)$$

Relaxivity determination

Relaxivities were determined using a field cycling relaxometer at NY Medical College over the frequency range 0.01 to 50 MHz. Relaxivity was determined for **5** in either pH 7.4 TBS (50 mM), human plasma, 10 mg mL^{-1} (30 μM) fibrinogen in TBS or 30 μM fibrin gel in TBS. The fibrin gel samples were prepared by first mixing appropriate amounts of fibrinogen stock solution (15–20 mg mL^{-1}), **5** stock and TBS to a total volume of 400 μL. To this solution was added 4 μL of a 2 M $CaCl_2$ solution and 2 μL of human thrombin (0.6 units). The resultant solution was vigorously mixed for 3 s and then incubated for 1 h at 37 °C to allow complete polymerization of the fibrinogen. 22 data point $1/T_1$ dispersions were recorded for either a 100 μM **5** solution in TBS, 50 μM **5** in 30 μM fibrin gel, 50 μM **5** in 30 μM fibrinogen solution, 100 μM **5** in human plasma, human plasma alone, 30 μM fibrinogen solution alone or 30 μM fibrin gel without compound. There are known to be two equivalent binding sites on fibrin for these peptides,[8] so the NMRD in fibrin gel was recorded under conditions where the [binding sites] > [**5**]. Based on the measured binding constant, under these conditions, **5** was 81% bound to fibrin. Compound concentration was determined from an ICP-MS analysis of the total Gd content and dividing by the number of Gds per molecule. Relaxivity was computed by subtracting the relaxation rate of the medium (TBS, plasma, fibrinogen or fibrin gel/TBS) from the relaxation rate of the gadolinium solution at each field strength and dividing the difference by the gadolinium concentration in millimoles.

Variable temperature O-17 NMR

$H_2{}^{17}O$ transverse relaxation rates were determined for a TBS buffer solution in the presence and absence of 11.75 mmolal **5** as a function of temperature (−6 to 92 °C) on a Varian Unity 300 NMR instrument operating at 40.6 MHz. Probe temperatures were determined from ethylene glycol or methanol chemical shift calibration curves. T_2 was determined by a CPMG pulse sequence and T_1 by inversion recovery. Data were analyzed as previously described.[18]

References

1 Y. S. Kim, Z. He, W. Y. Hsieh and S. Liu, *Bioconjugate Chem.*, 2007, **18**, 929–936.
2 S. Liu, *Chem. Soc. Rev.*, 2004, **33**, 445–461.
3 P. Caravan, *Acc. Chem. Res.*, 2009, **42**, 851–862.
4 C. Adessi and C. Soto, *Curr. Med. Chem.*, 2002, **9**, 963–978.
5 T. K. Sawyer, in *Peptide-Based Drug Design*, ed. M. D. Taylor and G. L. Amidon, American Chemical Society, Washington, 1995, pp. 387.
6 P. Caravan, B. Das, Q. Deng, S. Dumas, V. Jacques, S. K. Koerner, A. Kolodziej, R. J. Looby, W. C. Sun and Z. Zhang, *Chem. Commun.*, 2009, 430–432.
7 P. Caravan, B. Das, S. Dumas, F. H. Epstein, P. A. Helm, V. Jacques, S. Koerner, A. Kolodziej, L. Shen, W. C. Sun and Z. Zhang, *Angew. Chem., Int. Ed.*, 2007, **46**, 8171–8173.
8 S. Nair, A. F. Kolodziej, G. Bhole, M. T. Greenfield, T. J. McMurry and P. Caravan, *Angew. Chem., Int. Ed.*, 2008, **47**, 4918–4921.
9 K. Overoye-Chan, S. Koerner, R. J. Looby, A. F. Kolodziej, S. G. Zech, Q. Deng, J. M. Chasse, T. J. McMurry and P. Caravan, *J. Am. Chem. Soc.*, 2008, **130**, 6025–6039.
10 V. Amirbekian, J. G. Aguinaldo, S. Amirbekian, F. Hyafil, E. Vucic, M. Sirol, D. B. Weinreb, S. Le Greneur, E. Lancelot, C. Corot, E. A. Fisher, Z. S. Galis and Z. A. Fayad, *Radiology*, 2009, **251**, 429–438.
11 L. M. De León-Rodríguez, A. Ortiz, A. L. Weiner, S. Zhang, Z. Kovacs, T. Kodadek and A. D. Sherry, *J. Am. Chem. Soc.*, 2002, **124**, 3514–3515.

12 A. Morisco, A. Accardo, E. Gianolio, D. Tesauro, E. Benedetti and G. Morelli, *J. Pept. Sci.*, 2009, **15**, 242–250.
13 J. F. Poduslo, T. M. Wengenack, G. L. Curran, T. Wisniewski, E. M. Sigurdsson, S. I. Macura, B. J. Borowski and C. R. Jack, Jr, *Neurobiol. Dis.*, 2002, **11**, 315–329.
14 F. Ye, E. K. Jeong, Z. Jia, T. Yang, D. Parker and Z. R. Lu, *Bioconjugate Chem.*, 2008, **19**, 2300–2303.
15 P. Caravan, A. F. Kolodziej, J. M. Greenwood, S. Witte, R. J. Looby, Z. Zhang, M. Spiller, T. J. McMurry, R. M. Weisskoff and P. B. Graham, in *Proc. 10th ISMRM Scientific Meeting*, Honolulu, HI, USA, 2002, pp. 217.
16 Z. Zhang, S. Nair, X. Wang, A. F. Kolodziej, A. Case, P. Caravan, M. T. Greenfield, P. B. Graham and T. J. McMurry, in *Proc. 4th Soc. Mol. Imaging*, Cologne, Germany, 2005, p. 389.
17 M. Sirol, J. G. Aguinaldo, P. B. Graham, R. Weisskoff, R. Lauffer, G. Mizsei, I. Chereshnev, J. T. Fallon, E. Reis, V. Fuster, J. F. Toussaint and Z. A. Fayad, *Atherosclerosis*, 2005, **182**, 79–85.
18 P. Caravan, G. Parigi, J. M. Chasse, N. J. Cloutier, J. J. Ellison, R. B. Lauffer, C. Luchinat, S. A. McDermid, M. Spiller and T. J. McMurry, *Inorg. Chem.*, 2007, **46**, 6632–6639.
19 I. Bertini, C. Luchinat and G. Parigi, *Solution NMR of Paramagnetic Molecules*, Elsevier, Amsterdam, 2001.
20 D. H. Powell, O. M. Ni Dhubhghaill, D. Pubanz, L. Helm, Y. S. Lebedev, W. Schlaepfer and A. E. Merbach, *J. Am. Chem. Soc.*, 1996, **118**, 9333–9346.
21 G. Lipari and A. Szabo, *J. Am. Chem. Soc.*, 1982, **104**, 4546–4559.
22 E. Spuentrup, R. M. Botnar, A. J. Wiethoff, T. Ibrahim, S. Kelle, M. Katoh, M. Ozgun, E. Nagel, J. Vymazal, P. B. Graham, R. W. Gunther and D. Maintz, *Eur. Radiol.*, 2008, **18**, 1995–2005.
23 Z. Zhang, J. Amedio, P. Caravan, S. Dumas, A. Kolodziej and T. J. McMurry, Peptide-based multimeric targeted contrast agents, *US. Pat.*, US7,238,341 B2, issued July 3, 2007.
24 J. Graham and J. R. Harris, in *Cell Biology Protocols*, ed. J. R. Harris, J. Graham and D. Rickwood, Wiley and Sons, New York, 2008, pp. 88.
25 K. A. Moskowitz and A. Z. Budzynski, *Biochemistry*, 1994, **33**, 12937–12944.
26 S. Feng, C. Kasahara, R. J. Rickles and S. L. Schreiber, *Proc. Natl. Acad. Sci. U. S. A.*, 1995, **92**, 12408–12415.

